

ANGULAR DIAMETERS OF MAGELLANIC CLOUD PLANETARY NEBULAE. I. SPECKLE INTERFEROMETRY

P. R. WOOD, M. S. BESSELL, AND M. A. DOPITA

Mount Stromlo and Siding Spring Observatories, Institute of Advanced Studies, Australian National University

Received 1985 October 17; accepted 1986 May 29

ABSTRACT

Speckle interferometric angular diameters of Magellanic Cloud planetary nebulae are presented. The mass of ionized gas in each nebula has been derived from the angular diameter and published $H\beta$ line fluxes; the derived masses range from less than $0.006 M_{\odot}$ to greater than $0.19 M_{\odot}$. The planetary nebulae observed were, of necessity, the brightest in the Magellanic Clouds; consequently, they are all relatively small (diameter $\lesssim 0.13$ pc), young (age $\lesssim 1500$ yr), bright, and dense. They are almost certainly only partially ionized, so that the masses derived for the ionized parts of the nebula are lower limits to the total nebula mass. The properties of the Magellanic Cloud nebulae are compared with those of planetary nebulae at the Galactic center.

Subject headings: galaxies: Magellanic Clouds — interferometry — nebulae: planetary

I. INTRODUCTION

A problem which has long hindered accurate quantitative determinations of parameters such as mass, linear diameter, and age for Galactic planetary nebulae is the lack of an accurate distance scale for these objects. Current distance scales (e.g., Cahn and Kaler 1971; Cudworth 1974; Acker 1978; Maciel and Pottasch 1980; Daub 1982) vary by systematic factors of up to 2; the differences between the distance scales are even larger for optically thick objects. Hence, expansion ages (the ratio of linear radius to expansion velocity) are uncertain by factors of 2 or more, while masses, which vary as $d^{2.5}$ (where d is distance) in the most common method of mass determination (e.g., Seaton 1966), are uncertain by factors of $2^{2.5} = 5.7$ or more. Better methods of distance determination are clearly required for the Galactic planetary nebulae. With the increasing accuracy and complexity of stellar evolution calculations for the nuclei of planetary nebulae (e.g., Schonberner 1983; Iben 1984; Wood and Faulkner 1986), better observational constraints are required in order to distinguish between the many possible evolutionary scenarios. For example, accurate determinations of ages and masses of planetary nebulae, together with accurate effective temperatures and luminosities for the central stars, would tell us a great deal about the mode of planetary nebula ejection and about the mass ejected as a function of initial mass.

One way to overcome the problem of distance inaccuracy inherent in studies of Galactic planetary nebulae is to study the planetary nebulae in the Magellanic Clouds. However, here another problem arises: the angular diameters of all but the largest planetary nebulae in the Magellanic Clouds will be less than $1''$, so that the angular diameters can not, in general, be determined by direct imaging techniques. Since the angular diameter (ϕ) is needed in the formula for determining planetary nebula mass (M) from the $H\beta$ flux, with $M \propto \phi^{1.5}$, mass determinations for Cloud planetaries have not been possible in the past except for a few large nebulae with angular diameters measured by Jacoby (1980).

In order to obtain angular diameters for the smaller Magellanic Cloud planetary nebulae, techniques such as speckle interferometry are required. Here, we report results of the determination of angular diameters of Magellanic Cloud plan-

etary nebulae in the light of $[O III] \lambda 5007$ using a speckle interferometer on the Anglo-Australian Telescope (AAT). Because of the signal-to-noise (S/N) limitations pertaining to speckle interferometry (e.g. Dainty 1978; Walker 1979; Wood 1985), only the brightest of the Magellanic Cloud planetary nebulae can be studied in this way. In a subsequent paper, we will present results of a study of fainter (larger) nebulae using direct imaging techniques.

II. OBSERVATIONS AND DATA REDUCTION

The speckle observations were made on the AAT with a speckle device attached to the Cassegrain focus. The essential elements of this device (Wood 1985) are (1) a filter to isolate the $[O III] \lambda 5007$ line, (2) a lens (microscope objective) to enhance the image scale on the detector, and (3) a photon-counting detector (IPCS) which was run with a frame time of 16 ms and an area of 240×240 pixels. No atmospheric dispersion correction was included since the $[O III]$ line is so narrow in planetary nebulae that atmospheric dispersion is negligible. For point source standards, the filter used (24 \AA FWHM) was sufficiently narrow that atmospheric dispersion was not significant except at the largest zenith distances. At a zenith distance of 60° , atmospheric dispersion of the image is becoming comparable to the size of the diffraction limited image, but since the planetary nebulae we are studying are considerably larger than the diffraction limit, it was not necessary to compensate or correct for atmospheric dispersion. Most of the observations were made in $\sim 1''$ seeing with exposure times of 20–50 minutes.

The first step in data reduction was the calculation of the two-dimensional autocorrelation function (the histogram of vector differences between pairs of photons, summed over all pairs in each frame and over all frames). Frames containing ion events were not included in the data reduction. A typical autocorrelation function consists of the autocorrelation of the diffraction limited image of the object being observed superposed on a pedestal which corresponds to the autocorrelation of the seeing disk (e.g., Blazit *et al.* 1977). The most difficult part of the data reduction process is the determination of that part of the autocorrelation which belongs to the seeing disk. For extended objects, uncertainty in the determination of the

seeing disk component of the autocorrelation is the main factor which limits detectability, rather than photon noise, which limits the detection of binaries and objects of size comparable to the Airy disk.

The procedure we have used to remove the seeing disk is based on the cross-correlation method of Worden *et al.* (1977). The basis of this technique is the observation that the speckle patterns in two images separated in time by more than ~ 0.5 are uncorrelated. Therefore, if the vector crosscorrelation of two frames separated by ~ 0.5 is computed (where the vector cross-correlation is the histogram of the vector differences between all pairs of photons, one member of each pair being in the first frame and the other member being in the second frame), then the resulting cross-correlation will contain the seeing disk component of the autocorrelation of a single frame but no speckle component. In practice, this statement is not exactly true since atmospheric conditions may vary over time scales of ~ 0.5 , e.g., translation of the image can occur causing the cross correlation to be more spread out than the seeing disk component of the autocorrelation. However, by subtracting the cross-correlation (suitably scaled) from the autocorrelation, the major part of the seeing disk component of the autocorrelation can be removed, along with most of the effects of guiding errors and of overfilling of the detector by the seeing disk (the latter two problems introduce edge effects into the autocorrelation). In order to make an estimate of angular size, the residual of the autocorrelation of the program object is compared with a similar residual of the autocorrelation of a point source observed in the same part of the sky immediately before or after the program object.

The data reduction procedure we used is as follows (see Wood 1985 for further details):

1. Compute the cumulative vector autocorrelation $A(x, y)$ of all frames taken during observation of the program object.
2. At the same time, compute the vector cross-correlation of each frame with a frame taken t seconds previously (where $t \approx 0.5-1.0$ s). Add all such cross-correlations to produce the cumulative vector cross-correlation $C(x, y)$.
3. Compute the autocorrelation $A_{ps}(x, y)$ and cross correlation $C_{ps}(x, y)$ for the point source with which the program object is to be compared (a point source nearby in the sky observed immediately before or after the program object).
4. For the point source, find a constant α such that the function $B_{ps}(x, y) = A_{ps}(x, y) - \alpha C_{ps}(x, y)$ is approximately constant at positions more than a few Airy disk radii from the origin. The purpose of this procedure is to remove as much as possible of the seeing disk component of $A_{ps}(x, y)$; $B_{ps}(x, y)$ consists predominantly of the speckle component of $A_{ps}(x, y)$.
5. Using the value of α from the point source, $B(x, y)$ is calculated for the program object. A single value of α was generally found appropriate for all objects observed in one night.
6. The angular "size" of the program object is determined by comparing the azimuthally averaged autocorrelation residual $B(r)$ of the program object with the equivalent function $B_{ps}(r)$ of the comparison point source. In order to make this comparison, it is necessary to correctly scale the $B(r)$ functions of the two objects, yielding normalized functions $B'(r)$. The normalization factor by which $B(r)$ should be divided is the height of the seeing disk pedestal in the autocorrelation; this is because at low count rates the *ratio* of the heights of the speckle and seeing disk components in the autocorrelation is independent of both count rate and seeing conditions. (In con-

ditions where the seeing does not vary with time, the total number of speckle vectors in the autocorrelation is proportional to $n_f n(n-1)$, where n_f is the number of frames and n is the number of photons per frame; in this situation the normalized functions $B'(r) = B(r)/[n_f n(n-1)]$ can be compared.) The normalized, radial, residual autocorrelation functions $B'(r)$ of our objects are shown in Figure 1.

In order to make quantitative predictions from $B'(r)$, one can postulate models for the program objects, compute the autocorrelations of diffraction limited images of these models as observed with the AAT (including the central obscuration of the primary mirror), and compare them with observed values of $B'(r)$ after suitable normalization. Some model autocorrelations of uniform disks and a point source are shown in the first panel of Figure 1, normalized for direct comparison with the program objects. The autocorrelations shown have maxima at the origin, and they drop effectively to zero at a distance from the origin corresponding to the angular diameter of the object being observed. The models clearly show how the height of the normalized speckle component of the autocorrelation is reduced as the size of the object increases. To get an angular diameter for an object of size ~ 0.5 or greater requires not only high S/N data but, more importantly, it requires an ability to accurately remove the seeing disk component—a particularly difficult task. We do not believe that sizes greater than 0.5 can be reliably determined by the speckle technique.

There are two important features to be seen in the models in Figure 1: (1) the maximum distance out to which speckle power exists in the autocorrelation corresponds to the angular diameter of the object being observed (convolved with the Airy disk) and (2) relative to a point source, extended objects show a deficiency of power in the autocorrelation at distances less than $\sim 2-3$ Airy disk radii (7–11 pixels). In view of (1), we assume the size (diameter) of a program object to be the point at which $B'(r)$ intersects $B'_{ps}(r)$; eye-estimates of these intersection points are marked by arrows in Figure 1. Feature (2) above is an indicator of the presence of an extended object.

Although uniform disks are not often good representations of real planetary nebulae, features (1) and (2) are still valid generally. Real planetary nebulae are frequently knotty and may have a bright central star so that they will tend to have a point source component as well as an extended component in the autocorrelation. Other planetary nebulae have a ring structure and will exhibit an autocorrelation function $B'(r)$ with a peak at the position corresponding to the diameter of the ring.

For objects where the S/N is large enough, the two-dimensional residual autocorrelation function $B'(x, y)$ may be examined directly. An interesting example is shown in Figure 2. This Figure is the autocorrelation of the diffraction limited image of LMC 1. It is not possible to invert an autocorrelation to get back to a true image except in certain cases (for example, when the object has circular symmetry). However, in the case of LMC 1 there must be three, or possibly four, bright knots arranged in a triangular, or cross-shaped, pattern with the knots being separated by ~ 0.09 .

Finally, we make some comments on individual nebulae. SMC 2: the angular diameter seems well defined at 0.20 ; SMC 15: the angular diameter seems reasonably well defined at 0.15 ; LMC 1 has a knotty structure with knot separation ~ 0.09 , and a total angular diameter of 0.22 ; LMC 3: the angular diameter is defined as 0.22 (30 pixels), although an angular diameter of 0.28 (38 pixels) is also possible; LMC 47: this object shows the lack of power inside $\sim 2-3$ Airy disk radii

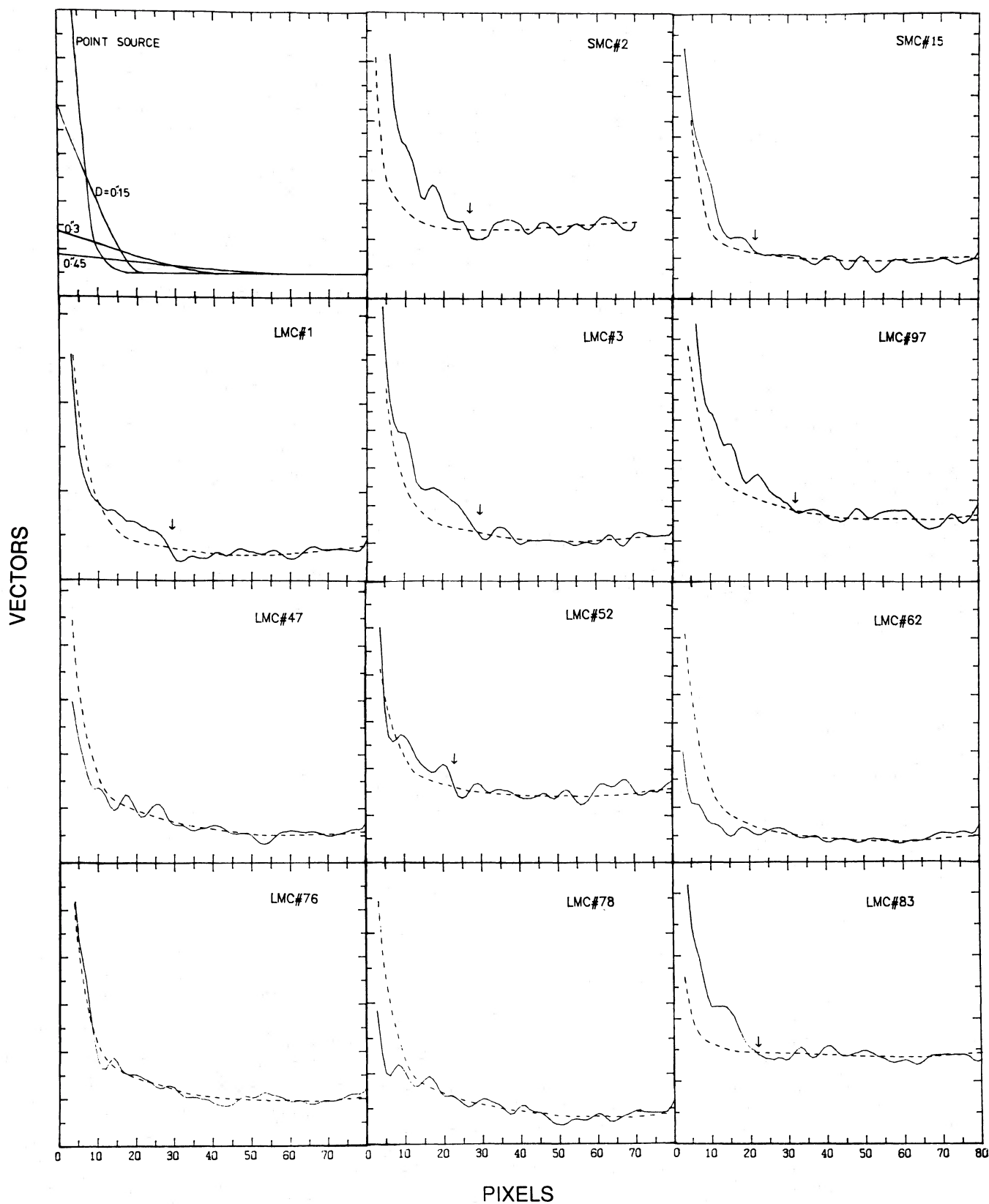


FIG. 1.—The azimuthally averaged autocorrelation functions $B'(r)$ of: model uniform disks of the angular diameters shown and of a point source (*first panel*) and Magellanic Cloud planetary nebulae (*remaining panels*). Most of the seeing disk component of each autocorrelation has been removed, as described in the text. The heights of the model curves have been normalized to be the same as those of the program objects. For each of the program objects, the autocorrelation function $B'_{ps}(r)$ of the comparison point source is shown as a dotted line. Arrows indicate the diameters adopted for the Magellanic Cloud planetaries. Pixel size is $0''.0073$ in all panels except LMC 83 where it is $0''.0146$. The inner few pixels are dominated by the autocorrelation of single photon events.

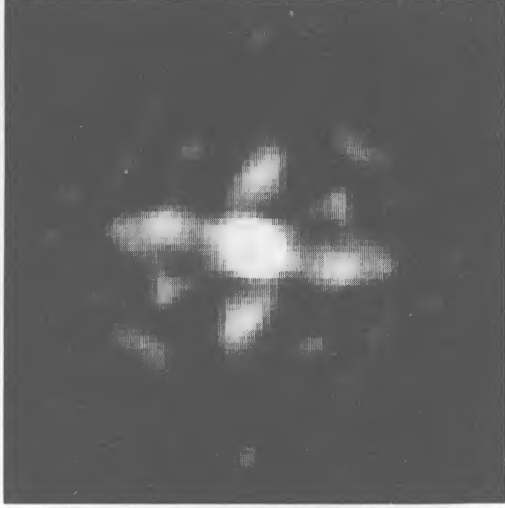


FIG. 2.—The full two-dimensional autocorrelation function of LMC 1. The figure is $0''.5$ across and the N-S direction is vertical. This form of autocorrelation results from an object with 3 or 4 bright knots separated by $\sim 0''.09$.

(relative to the comparison point source) and the lack of excess power beyond this point, which is characteristic of an extended source ($>0''.5$ diameter); LMC 52: the power excess out to pixel 22 indicates an angular diameter of $0''.16$; LMC 62: this object shows the deficiency of power within a few Airy disk radii of the origin which is characteristic of an extended source; LMC 76: the autocorrelation of this object shows close agreement with that of the comparison point source; LMC 78: this object shows the deficiency of power within a few Airy disk radii of the origin which is characteristic of an extended source; LMC 83: the angular diameter is well defined at $0''.32$ (pixel size is $0''.0146$ for this object compared with $0''.0073$ for the other objects); and LMC 97: the angular diameter seems well defined at $0''.23$.

III. RESULTS

The results of the present investigation are given in Table 1. The contents of the table are as follows: column (1), the planetary nebula identification using the numbering scheme of Sand-

TABLE 1
PLANETARY NEBULA PARAMETERS

Number (1)	ϕ (2)	D (pc) (3)	$\log F\beta$ (4)	Excitation Class (5)	M/M_{\odot} (6)	ϕ_{N_e} (7)	Age (yr) (8)
SMC							
2	$0''.20$	0.064	-12.69	6	0.06	$0''.33$	940
15	0.15	0.048	-12.44	2-4	0.05	0.12	1500
LMC							
1	0.22	0.055	-12.47	4	0.05	0.23	840
3	0.22	0.055
47	>0.5	>0.126	-12.51	6-7	>0.15	0.53	>1300
52	0.16	0.040	-12.71	5	0.02	1.00	510
62	>0.5	>0.126	-12.30	6	>0.19	0.56	>1400
76	<0.06	<0.015	-12.53	3	<0.006	0.22	<280
78	>0.5	>0.126	-12.60	6	>0.14	0.50	>1390
83	0.32	0.081	-12.65	8-9	0.07	0.72	360
97	0.23	0.058	-12.82	8-9	0.03	...	480

NOTE.—Identification numbers from Sanduleak, MacConnell, and Philip 1978.

uleak, MacConnell, and Philip (1978); column (2), the angular diameter ϕ in seconds of arc; column (3), the linear diameter in pc; column (4), the logarithm of the $H\beta$ flux ($\text{ergs cm}^{-2} \text{s}^{-1}$) from various sources in the literature (Webster 1969, 1976; Aller 1983); column (5), the excitation class from Morgan (1984); column (6), the mass M of ionized gas in the nebula, assuming a helium to hydrogen number ratio of 0.1; column (7), the angular diameter ϕ_{N_e} the nebula would be expected to have given the $H\beta$ flux and the electron density from the $[\text{O II}] \lambda 3729/\lambda 3726$ ratio; and column (8), the expansion age (radius divided by expansion velocity).

The ionized masses were computed using the formula (e.g., Webster 1976)

$$M/M_{\odot} = 47.3d^{2.5}(\epsilon F\beta)^{0.5}\phi^{1.5}, \quad (1)$$

where d is the distance to the planetary nebula in kpc ($d = 52$ kpc has been adopted for the LMC and $d = 66$ kpc for the SMC), $F\beta$ is in $\text{ergs cm}^{-2} \text{s}^{-1}$, ϕ is in arc seconds, and ϵ is the filling factor ($\epsilon = 0.7$ has been adopted). An electron temperature $T_e = 10^4$ K has been assumed in the emitting region. An angular diameter ϕ_{N_e} can be estimated from $F\beta$ and the electron density N_e (cm^{-3}) obtained from forbidden-line ratios using the formula given by Seaton (1966)

$$\phi_{N_e} = 8.1 \times 10^6 [F\beta/(\epsilon d N_e^2)]^{1/3}. \quad (2)$$

Once again, $T_e = 10^4$ K has been assumed. Values of N_e were derived from the $[\text{O II}] \lambda 3729/\lambda 3726$ ratios obtained by Webster (1976) and by Dopita, Ford, and Webster (1985b); the computer code MAPPINGS (Binette, Dopita, and Tuohy 1985) was used to generate the relation between N_e and the $[\text{O II}] \lambda 3729/\lambda 3726$ ratio.

In general, the angular diameters ϕ estimated from Figure 1 should be accurate to better than 20%, with the uncertainty increasing with nebular angular size. An uncertainty of 20% in ϕ will lead to a corresponding uncertainty of 30% in derived nebula mass. The uncertainty in the distance moduli to the Magellanic Clouds could lead to systematic errors of similar size in the derived masses, e.g., an overestimate of 0.2 in distance modulus will produce masses too large by a factor of ~ 1.26 .

IV. DISCUSSION

The planetary nebula masses derived above have values from less than $0.005 M_{\odot}$ to more than $0.19 M_{\odot}$, with a mean value of $0.08 M_{\odot}$. As noted earlier, the objects we have observed are, of necessity, the brightest of the planetary nebulae in the Magellanic Clouds in $H\beta$ flux; they are ~ 10 times brighter than typical local Galactic planetaries (compare the fluxes of our sample with Fig. 5 of Pottasch 1983). Among the nearby planetaries, the brighter nebulae are optically thick (Pottasch 1983), so that the objects we have observed in the Magellanic Clouds are almost certainly optically thick also. This suggestion is consistent with the fact that the linear diameters of the Cloud planetaries are relatively small (0.015–0.13 pc), as are the expansion ages (150–1600 yr, using expansion velocities derived from the relation between expansion velocity and excitation class given by Dopita *et al.* 1985, together with expansion velocities measured for SMC 2 and 15 by Dopita *et al.* 1985 and for LMC 83 by Dopita, Ford, and Webster 1985a); the electron densities are also relatively large, ranging from $N_e \approx 0.2 \times 10^4$ to $\sim 5 \times 10^4 \text{ cm}^{-3}$ with a mean of $\sim 1.3 \times 10^4 \text{ cm}^{-3}$. It therefore appears that the bright Magellanic Cloud planetary nebulae that we have observed are

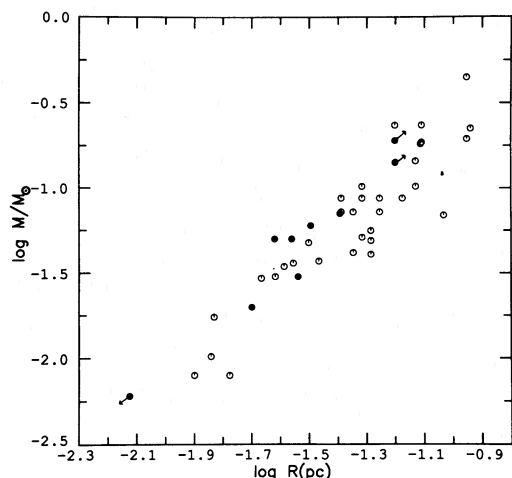


FIG. 3.—Nebular mass plotted against nebular radius for objects in the Magellanic Clouds (filled circles) and in the Galactic Center (open circles). A distance of 8.5 kpc to the Galactic center has been assumed. Data for the Galactic center objects comes from Gathier *et al.* (1983).

young, dense, and optically thick. In these circumstances, the ionized masses that we have derived will be lower limits to the total (ionized plus unionized) nebula masses.

We will now compare our results for Magellanic Cloud planetary nebulae with the results of Gathier *et al.* (1983) for Galactic center planetary nebulae. In Figure 3, the relation between ionized mass and radius is shown for our Magellanic Cloud nebulae and for Galactic center nebulae (Gathier *et al.* 1983). For both groups of nebulae, a relation of the form $M \propto R^{1.5}$ seems to hold with a similar zero point in each case. Pottasch (1980) found that nearby planetary nebulae obey a mass-radius relation of slope similar to that of the Galactic center planetary nebulae but with a different zero point (however, the zero point for local planetaries is uncertain because of the well-known difficulties with distance determinations for local planetaries).

It should be noted that a relation $M \approx R^{1.5}$ would be obtained for our objects regardless of the radii found, since all objects have similar fluxes (to within a factor of 3) and the ionized mass $M \propto \phi^{1.5}(F\beta)^{0.5}$. Note that the zero point of the Cloud and Galactic center (M, R) relations is unaffected by errors in angular diameter (errors in angular diameter affect only the range in M and R exhibited by the nebulae).

Maciel and Pottasch (1980) exploited a (M, R) relation in order to derive a distance scale for planetary nebulae and Daub (1982) used essentially the same approach. In principle, the relation in Figure 3 could be exploited in a similar way. However, because the nebulae in Figure 3 are the brightest in the Magellanic Clouds and at the Galactic center, the (M, R) relation will not be obeyed by an “average” planetary nebula. An application of the relation in Figure 3 would indicate distances ~ 3 times those derived from Daub’s relation for optically thick nebulae. The relation $M \approx R^{1.5}$ found in Figure 3 corresponds to nebulae having a constant $H\beta$ flux, as assumed for optically thick nebulae by Acker (1978); the mean intrinsic flux implied by Figure 3 is ~ 4 times that adopted by Acker, consistent with the fact that the nebulae in Figure 3 are among the most intrinsically luminous. It is clear from these results that the Acker and Daub relations do not apply to all optically thick nebulae.

Both the Magellanic Cloud and Galactic center planetary nebulae occupy similar large mass ranges in Figure 3. Individual planetary nebulae in the Galaxy also appear to exhibit a large range in ionized mass from $\sim 10^{-3} M_{\odot}$ to $\sim 1 M_{\odot}$ (Pottasch 1983); the masses derived here occupy a smaller range due to the absence of the most massive nebulae with $M \approx M_{\odot}$. These nebulae would be fully ionized, large, and faint, and are not suitable for diameter measurement using speckle techniques. Their study by direct imaging techniques will be discussed in the second paper in this series.

V. SUMMARY

Speckle interferometric angular diameters have been measured for a number of the brightest planetary nebulae in the Magellanic Clouds. These objects are young, dense, and only partially ionized. They appear to obey an (ionized mass, radius) relation similar to that of nebulae at the Galactic center. In order to obtain a complete sample of Magellanic Cloud nebulae including the older, larger, fainter, and fully ionized nebulae, direct imaging techniques are needed to supplement the speckle measurements of angular diameter.

We are grateful to the AAO for allotting time for the development of the speckle system, and to the staff of the AAO for their assistance at the telescope. In particular, we would like to thank C. McCowage for modifying the IPCS hardware, for his very generous assistance with operation of the speckle system, and for his continued interest.

REFERENCES

- Acker, A. 1978, *Astr. Ap., Suppl.*, **33**, 367.
 Aller, L. H. 1983, *Ap. J.*, **273**, 590.
 Binette, L., Dopita, M. A., and Tuohy, I. R. 1985, *Ap. J.*, **297**, 476.
 Blazit, A., Bonneau, D., Koechlin, L., and Labeyrie, A. 1977, *Ap. J. (Letters)*, **214**, L79.
 Cahn, J. H., and Kaler, J. B. 1971, *Ap. J. Suppl.*, **22**, 319.
 Cudworth, K. M. 1974, *A.J.*, **79**, 1384.
 Dainty, J. C. 1978, *M.N.R.A.S.*, **183**, 223.
 Daub, C. T. 1982, *Ap. J.*, **260**, 612.
 Dopita, M. A., Ford, H. C., Lawrence, C. J., and Webster, B. L. 1985, *Ap. J.*, **296**, 390.
 Dopita, M. A., Ford, H. C., and Webster, B. L. 1985a, *Ap. J.*, **297**, 593.
 ———. 1985b, private communication.
 Gathier, R., Pottasch, S. R., Goss, W. M., and van Gorkom, J. H. 1983, *Astr. Ap.*, **128**, 325.
 Iben, I. 1984, *Ap. J.*, **277**, 333.
 Jacoby G. H. 1980, *Ap. J. Suppl.*, **42**, 1.
 Maciel, W. J., and Pottasch, S. R. 1980, *Astr. Ap.*, **88**, 1.
 Morgan, D. H. 1984, *M.N.R.A.S.*, **208**, 633.
 Pottasch, S. R. 1980, *Astr. Ap.*, **89**, 336.
 ———. 1983, in *IAU Symposium 103, Planetary Nebulae*, ed. D. R. Flower (Dordrecht: Reidel), p. 391.
 Sanduleak, N., MacConnell, D. J., and Philip, A. G. D. 1978, *Pub. A.S.P.*, **90**, 621.
 Schonberner, D. 1983, *Ap. J.*, **272**, 708.
 Seaton, M. J. 1966, *M.N.R.A.S.*, **132**, 113.
 Walker, J. G. 1979, *Opt. Comm.*, **29**, 273.
 Webster, B. L. 1969, *M.N.R.A.S.*, **143**, 79.
 ———. 1976, *M.N.R.A.S.*, **174**, 513.
 Wood, P. R. 1985, *Proc. Astr. Soc. Australia*, **6**, 120.
 Wood, P. R., and Faulkner, D. J. 1986, *Ap. J.*, **307**, 659.
 Worden, S. P., Stein, M. K., Schmidt, G. D., and Angel, J. R. P. 1977, *Icarus*, **32**, 450.